

An effective finite element approach for soil-structure analysis in the time-domain

L. Lehmann[†]

*Institute of Applied Mechanics, Technical University of Braunschweig, Spielmannstr. 11,
D-38106 Braunschweig, Germany*

(Received December 28, 2004, Accepted August 10, 2005)

Abstract. In this study, a complete analysis of soil-structure interaction problems is presented which includes a modelling of the near surrounding of the building (near-field) and a special description of the wave propagation process in larger distances (far-field). In order to reduce the computational effort which can be very high for time domain analysis of wave propagation problems, a special approach based on similarity transformation of the infinite domain on the near-field/far-field interface is applied for the wave radiation of the far-field. The near-field is discretised with standard Finite Elements, which also allows to introduce non-linear material behaviour. In this paper, a new approach to calculate the involved convolution integrals is presented. This approximation in time leads to a dramatically reduced computational effort for long simulation times, while the accuracy of the method is not affected. Finally, some benchmark examples are presented, which are compared to a coupled Finite Element/Boundary Element approach. The results are in excellent agreement with those of the coupled Finite Element/ Boundary Element procedure, while the accuracy is not reduced. Furthermore, the presented approach is easy to incorporate in any Finite Element code, so the practical relevance is high.

Key words: soil-structure interaction; time domain; finite element method; scaled boundary finite element method; coupled analysis.

1. Introduction

The various numerical methods, developed for the analysis of dynamic soil-structure interaction during the last years, can be classified into two main groups: the direct method and the substructure method (Antes and Spyarakos 1997).

Following the direct method, the structure and a finite, bounded soil zone adjacent to the structure, called near-field, are modelled by the Finite Element Method (FEM). The effect of the surrounding unbounded soil (called far-field) is approximated by imposing transmitting boundary conditions along the near-field/far-field interface. The simplest transmitting boundaries are the viscous boundaries (Lysmer and Kuhlmeyer 1969) which are simple dashpots. Other local, non-consistent boundaries (Engquist and Majda 1977, Liao and Wong 1984) and several other types of transmitting boundaries, e.g., boundaries based on rational transfer functions (Weber 1994), or Infinite Elements (Bettess 1992) have been proposed.

[†] Dr. -Ing., E-mail: lutz-o.lehmann@tu-bs.de

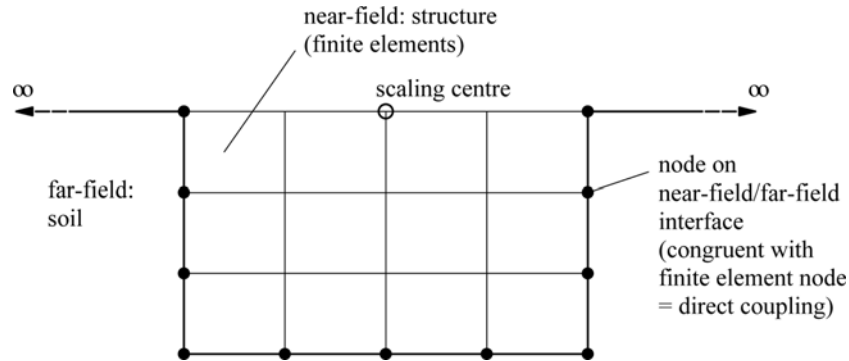


Fig. 1 Structure-soil-system: Discretisation scheme

Following the substructure method, the soil-structure system is divided into two parts: the structure (which may also include some portion of the soil) and the unbounded soil. These substructures are connected by a soil-structure interface, also called near-field/far-field interface, see Fig. 1. The unbounded soil is assumed to behave linear but in the near-field non-linearities can be included. So not only non-linear effects of the building itself can be included in the analysis, but also non-linear material behaviour of the soil adjacent to the structure (near-field). The reaction of the unbounded soil on the general soil-structure interface is represented by a boundary condition in the form of a force-displacement relationship which is global in space and time.

Based on the substructure method, hybrid methods (also referred as coupling methods) have been developed where the near-field is analysed by the FEM while the unbounded soil (near-field) is modelled by a different numerical method, which takes into account the influence of the infinite half-space, i.e., the Boundary Element Method (BEM). The BEM is a powerful procedure for modelling the unbounded medium since only the boundary of the unbounded medium is discretised so that the spatial dimension is reduced by one, see, e.g., Estorff and Firuziaan (2000). But the direct coupling of FEM and BEM usually destroys the structure of the system matrix, therefore the system of equations can not be solved effectively. It should be mentioned that the use of Symmetric Galerkin BEM avoids the problem of non-symmetric system matrices (see, e.g., Bonnet *et al.* 1998), but due to the appearance of double integrals, the computational costs to build the symmetric system matrix is increased. Also, fast multipole BEM is becoming a more and more popular method for getting “fast” solutions of the problem, see, e.g., Coifman *et al.* (1993) or Nishimura (2002).

In this paper, a hybrid method (substructure method) is used as well where the near-field is analysed with the FEM, while the unbounded soil is modelled by special finite elements, based on a similarity transformation, referred as cloning algorithm, see, Dasgupta (1982), Consistent Infinitesimal Finite-Element Cell Method, Song and Wolf (1995, 1996a, 1996b, 1997), Wolf and Song (1996), or Scaled Boundary Finite Element Method (SBFEM), Wolf (2003). Further developments have been made to the SBFEM, i.e., by Deeks and Wolf (2002), Crouch and Bennett (2000), Lehmann *et al.* (2004). The scaled boundary finite elements are building the near-field/far-field interface, so (like the BEM) they reduce the spatial dimension of the problem by one as well.

A realistic modelling of the situation next to the building is certainly possible by using the FEM. There, almost no restrictions regarding geometry and loading have to be considered. Moreover, different element types and material properties including non-linear material, see, i.e., Zienkiewicz

(1991) can be easily introduced in the numerical model.

In the analysis of soil-structure interaction effects, the correct modelling of the geometric radiation damping, i.e., the propagation of waves to infinity is essential for dynamic calculations. In order to reduce the computational effort which can be very high for long simulation times of transient analyses of soil-structure problems with a large number of degrees of freedom, an approximation in time for the similarity approach is introduced in this paper.

2. Governing equations

A summary of the governing equations of linear-elastic theory, including the equation of motion, with special respect to the time-domain is given.

2.1 Three-dimensional elasto-dynamics

In the following, the constitutive equations of linear theory for elastic materials are repeated briefly. Detailed explanations can be found, e.g., in the books of Gould (1994), or Eringen and Suhubi (1975). The vector of stress states $\boldsymbol{\sigma}^T = [\sigma_x \ \sigma_y \ \sigma_z \ \tau_{xy} \ \tau_{xz} \ \tau_{yz}]$ is combined via Hooke's law with the vector of strain states, $\boldsymbol{\varepsilon}^T = [\varepsilon_x \ \varepsilon_y \ \varepsilon_z \ 2\varepsilon_{xy} \ 2\varepsilon_{xz} \ 2\varepsilon_{yz}]$ as

$$\boldsymbol{\sigma} = \mathbf{D}\boldsymbol{\varepsilon} \quad (1)$$

Where \mathbf{D} is the elasticity matrix which may be stated for isotropic or anisotropic material.

For linear theory, the strain tensor is defined by the strain-displacement relationship

$$\boldsymbol{\varepsilon} = \mathbf{L}\mathbf{u} \quad (2)$$

with the differential operator \mathbf{L} given in its transposed form by:

$$\mathbf{L}^T = \begin{bmatrix} \frac{\partial}{\partial x} & 0 & 0 & \frac{\partial}{\partial y} & \frac{\partial}{\partial z} & 0 \\ 0 & \frac{\partial}{\partial y} & 0 & \frac{\partial}{\partial x} & 0 & \frac{\partial}{\partial z} \\ 0 & 0 & \frac{\partial}{\partial z} & 0 & \frac{\partial}{\partial x} & \frac{\partial}{\partial y} \end{bmatrix} \quad (3)$$

Applying this operator (Eq. (3)) on $\boldsymbol{\sigma}$, the dynamic equilibrium reads in the frequency domain:

$$\mathbf{L}^T \hat{\boldsymbol{\sigma}}(t) + \hat{\mathbf{b}}(t) + \omega^2 \rho \hat{\mathbf{u}} = \mathbf{0} \quad (4)$$

where $\hat{\boldsymbol{\sigma}}$, $\hat{\mathbf{b}}$, and $\hat{\mathbf{u}}$ stand for the spatial-dependent amplitudes of stresses, body forces, and displacements, respectively, and means the material density, while the equation of motion in the time domain is given by:

$$\mathbf{L}^T \boldsymbol{\sigma}(t) + \mathbf{b}(t) - \rho \ddot{\mathbf{u}}(t) = \mathbf{0} \quad (5)$$

where, now, all states, i.e., the stresses $\boldsymbol{\sigma}(t)$, the body loads $\mathbf{b}(t)$ and the accelerations $\ddot{\mathbf{u}}(t)$ are time-dependent.

2.2 FEM equations

Eq. (5) represents the equation of motion in the time domain for a general case. If one divides the domain in a near-field and a far-field part (see Fig. 1), and introduces a time-dependent interaction force vector $\mathbf{r}_b(t)$ (which represents the influence of the infinite domain) on the near-field/far-field interface, the equation of motion can be rewritten, see, e.g., Crouch and Bennett (2000):

$$\begin{bmatrix} \mathbf{K}_{ss} & \mathbf{K}_{sb} \\ \mathbf{K}_{bs} & \mathbf{K}_{bb} \end{bmatrix} \begin{bmatrix} \mathbf{u}_s(t) \\ \mathbf{u}_b(t) \end{bmatrix} + \begin{bmatrix} \mathbf{M}_{ss} & \mathbf{M}_{sb} \\ \mathbf{M}_{bs} & \mathbf{M}_{bb} + \gamma \Delta t \mathbf{M}_0^\infty \end{bmatrix} \begin{bmatrix} \ddot{\mathbf{u}}_s(t) \\ \ddot{\mathbf{u}}_b(t) \end{bmatrix} = \begin{bmatrix} \mathbf{p}_s(t) \\ \mathbf{p}_b(t) - \mathbf{r}_b(t) \end{bmatrix} \quad (6)$$

where the mass matrix \mathbf{M} , the stiffness matrix \mathbf{K} , and the node value vectors of the displacements \mathbf{u} and accelerations $\ddot{\mathbf{u}}$, respectively, are subdivided corresponding to the location of the nodes, i.e., the subscript b denotes the nodes on the soil-structure interface (boundary) and the subscript s the remaining nodes of the structure. On the right hand side of Eq. (6), $\mathbf{p}(t)$ is the vector of external forces.

When the interaction force vector $\mathbf{r}_b(t)$ is determined, the dynamic response of the structure can be obtained from Eq. (6) by using direct integration schemes, such as the Hilber-Hugh-Taylor implicit time integration scheme.

In the substructure method, the interaction forces on the near-field/far-field interface are given by the convolution integral

$$\mathbf{r}_b(t) = \int_0^t \mathbf{M}_\infty(t-\tau) \ddot{\mathbf{u}}_b(\tau) d\tau \quad (7)$$

where $\mathbf{M}_\infty(t)$ is the acceleration unit-impulse response matrix. In the next section it will be shown, how to perform an effective calculation of this convolution integral.

To determine the acceleration unit-impulse matrices $\mathbf{M}^\infty(t_i)$ at discrete time t_i , a concept of geometric similarity is used in conjunction with the standard approach of assembling finite elements. Consider the case of a structure modelled by conventional finite elements (see Fig. 1). A local portion of the soil would also be included in this part of the model. The far-field lies outside the finite element mesh representing the local soil and the structure. In an approach based on the concept of similarity, as in the SBFEM (Wolf and Song 1996), the geometry is described by a finite element discretisation with local coordinates η , ζ on the boundary (two dimensional finite elements representing the far-field/near-field interface of a three-dimensional problem) and a radial coordinate ξ containing also a scaling factor. This scaled boundary coordinate system is related to the Cartesian coordinate system (x, y, z) by the so-called scaled boundary transformation, which actually describes similarity.

The axes η and ζ lay in the circumferential directions (on the boundary) while the third coordinate ξ measures the distance from the scaling centre 0, being defined as $\xi = 1$ when crossing the boundary (see Fig. 2).

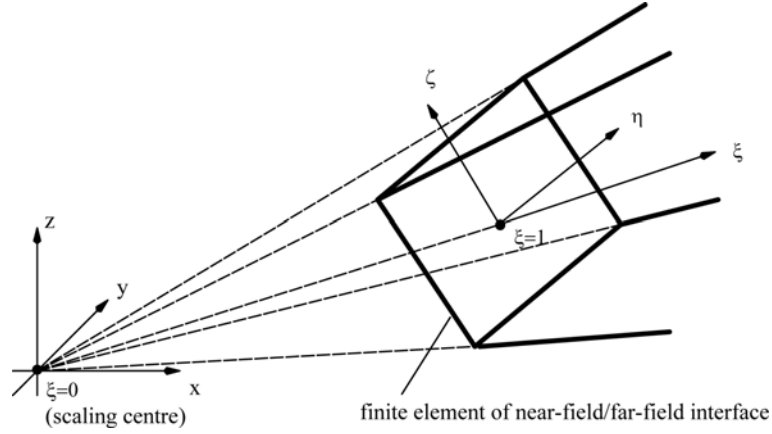


Fig. 2 Scaled boundary transformation for three dimensional problems: finite element and coordinate system

This scaled boundary coordinate system permits a numerical treatment in the circumferential directions η , ζ based on a weighted residual technique, as in the theory of finite elements. Thereby, the partial differential equations will be transformed into ordinary differential equations in the radial coordinate ξ , where their coefficients are determined by the Finite Element approximation in the circumferential directions.

For an unbounded medium, the radial coordinate ξ points from the boundary towards infinity (see Fig. 2), where the boundary condition at infinity (radiation condition) can be incorporated in the analytical solution.

3. Approximation in time

The calculation of the interaction force vector on the near-field/far-field interface for long simulation periods is computer-time consuming. In the following, a simple approximation algorithm is elaborated which leads to a reduction of computational effort without losing accuracy, see, Lehmann (2003) for two-dimensional problems, and Lehmann (2004) for a three-dimensional analysis.

3.1 Forces on the near-field/far-field interface

The forces $\mathbf{r}_b(t)$ are given by the convolution integral, see Eq. (7). To be able to treat this integral numerically, it is necessary to approximate this integral in respect to time by a time discretisation. If we assume a piecewise constant approximation of the acceleration unit impulse response matrix, i.e.,

$$\mathbf{M}_\infty(t) = \begin{cases} \mathbf{M}_0^\infty & t \in [0; \Delta t] \\ \mathbf{M}_1^\infty & t \in [\Delta t; 2\Delta t] \\ \vdots & \vdots \\ \mathbf{M}_{n-1}^\infty & t \in [(n-1)\Delta t; n\Delta t] \end{cases} \quad (8)$$

we get the discrete form of Eq. (7):

$$\mathbf{r}_n = \sum_{j=1}^n \mathbf{M}_{n-j}^{\infty} \int_{(j-1)\Delta t}^{j\Delta t} \ddot{\mathbf{u}}(\tau) d\tau = \sum_{j=1}^n \mathbf{M}_{n-j}^{\infty} (\dot{\mathbf{u}}_j - \dot{\mathbf{u}}_{j-1}) \quad (9)$$

Introducing the γ -parameter of the Hilber-Hughes-Taylor implicit time integration scheme, and separating the unknown acceleration vector $\ddot{\mathbf{u}}_n$, the calculation of \mathbf{r}_n can be performed with the following equation:

$$\mathbf{r}_n = \gamma\Delta t \mathbf{M}_0^{\infty} \ddot{\mathbf{u}}_n + \sum_{j=1}^{n-1} \mathbf{M}_{n-j}^{\infty} (\dot{\mathbf{u}}_j - \dot{\mathbf{u}}_{j-1}) = \gamma\Delta t \mathbf{M}_0^{\infty} \ddot{\mathbf{u}}_n + \tilde{\mathbf{r}}_n \quad (10)$$

For large n , i.e., long simulation time the direct solution of Eq. (10) is very time consuming, see Crouch and Bennett (2000). Therefore, an approximation in time is presented in the next subsection which leads to a recursive algorithm.

3.2 Recursive algorithm

A closer look at the acceleration unit impulse matrix \mathbf{M}^{∞} shows that the entries of matrices $\mathbf{M}^{\infty}(t_1), \mathbf{M}^{\infty}(t_2), \dots$ behave linear from a certain time-step t_m (see Fig. 3).

Hence, the acceleration unit impulse matrix can be decomposed (from time-step t_m on) as

$$\mathbf{M}^{\infty}(t_i) = \mathbf{T}^{\infty} t_i + \mathbf{C}^{\infty} \quad (11)$$

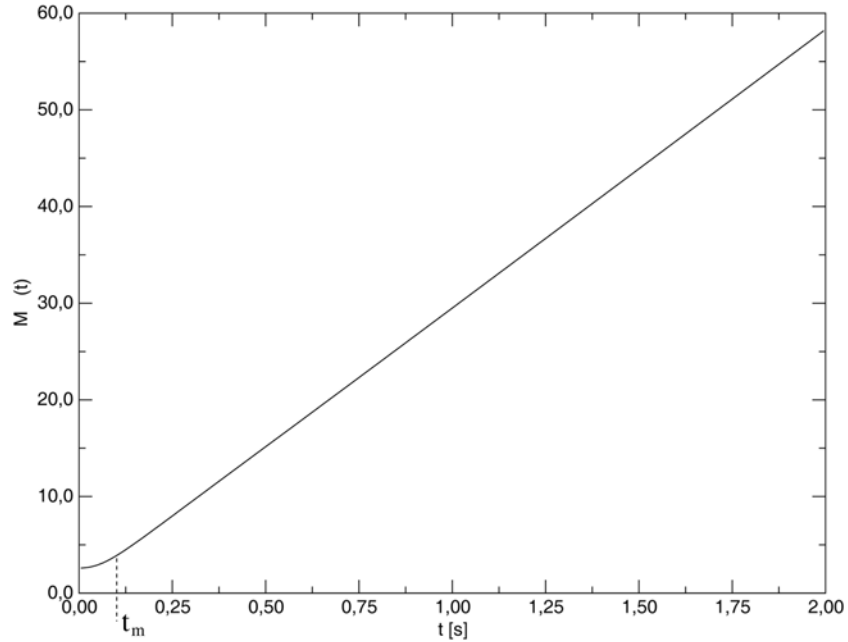


Fig. 3 Development of a matrix entry on the main diagonal of a unit impulse influence matrix over time-step

with the matrix T^∞ of gradients $(\Delta \mathbf{M}^\infty / \Delta t)$ and the constant matrix \mathbf{C}^∞ . For equidistant time-steps $t_i = i\Delta t$, the calculation of \mathbf{T}^∞ is reduced to

$$\mathbf{T}^\infty = (M_{m+1}^\infty - M_m^\infty) \quad \text{with} \quad \mathbf{M}_m^\infty = \mathbf{M}^\infty(t_m) \quad (12)$$

If a linear behaviour of matrix entries of \mathbf{M}^∞ is assumed, $\tilde{\mathbf{r}}_n$ of Eq. (10) can be divided in a non-linear term (for time-steps t_i , $0 \leq i \leq m$) and a linear term (time-steps t_i , $i > m$):

$$\begin{aligned} \tilde{\mathbf{r}}_n &= \tilde{\mathbf{r}}_n^{lin} + \tilde{\mathbf{r}}_n^{nonlin} \\ \tilde{\mathbf{r}}_n &= \sum_{j=1}^{n+1-m} M_{n-j+1}^\infty (\dot{\mathbf{u}}_j - \dot{\mathbf{u}}_{j-1}) + \sum_{j=n+2-m}^{n-1} M_{n-j+1}^\infty (\dot{\mathbf{u}}_j - \dot{\mathbf{u}}_{j-1}) \end{aligned} \quad (13)$$

With Eq. (11), the linear part of Eq. (13) can be written as

$$\begin{aligned} \tilde{\mathbf{r}}_n^{lin} &= \sum_{j=1}^{n+1-m} [\mathbf{T}^\infty(n-j+1) + \mathbf{C}^\infty] (\dot{\mathbf{u}}_j - \dot{\mathbf{u}}_{j-1}) \\ \tilde{\mathbf{r}}_n^{lin} &= [\mathbf{T}^\infty m + \mathbf{C}^\infty] (\dot{\mathbf{u}}_{n+1-m} - \dot{\mathbf{u}}_{n-m}) + \sum_{j=1}^{n-m} [\mathbf{T}^\infty(n-j+1) + \mathbf{C}^\infty] (\dot{\mathbf{u}}_j - \dot{\mathbf{u}}_{j-1}) \end{aligned} \quad (14)$$

$$\tilde{\mathbf{r}}_n^{lin} = \mathbf{M}_m^\infty (\dot{\mathbf{u}}_{n+1-m} - \dot{\mathbf{u}}_{n-m}) + \sum_{j=1}^{n-m} [\mathbf{T}^\infty(n-j+1) + \mathbf{C}^\infty] (\dot{\mathbf{u}}_j - \dot{\mathbf{u}}_{j-1})$$

For a recursive algorithm, $\tilde{\mathbf{r}}_{n-1}^{lin}$ is needed:

$$\tilde{\mathbf{r}}_{n-1}^{lin} = \sum_{j=1}^{n-m} [\mathbf{T}^\infty(n-j) + \mathbf{C}^\infty] (\dot{\mathbf{u}}_j - \dot{\mathbf{u}}_{j-1}) \quad (15)$$

With this equation, one can rewrite the difference $\tilde{\mathbf{r}}_n^{lin} - \tilde{\mathbf{r}}_{n-1}^{lin}$ and gets finally the recursive formulation:

$$\tilde{\mathbf{r}}_n^{lin} = \tilde{\mathbf{r}}_{n-1}^{lin} + \mathbf{M}_m^\infty (\dot{\mathbf{u}}_{n+1-m} - \dot{\mathbf{u}}_{n-m}) + \mathbf{T}^\infty (\dot{\mathbf{u}}_{n-m} - \dot{\mathbf{u}}_0) \quad (16)$$

So, the necessary operations for n time-steps are reduced (with *dof*: degrees of freedom) from

$$O(n) = \frac{3}{2} \text{dof}^2 n^2 \quad (17)$$

for the direct calculation to

$$O(m) = O(\psi)O(n) = 3 \text{dof}^2 nm - \frac{3}{2} \text{dof}^2 m^2 \quad \text{with} \quad \psi = \frac{m}{n} \quad (18)$$

The computational effort $O(\psi)$ in dependence on $\psi = m/n$ is shown in Fig. 4, e.g., when $n = 5000$ time-steps shall be calculated, one finds $m = 500$, $\psi = 0.1$ and $O(\psi) = 0.19$. Hence, for this example the reduction of necessary operation is 81%.

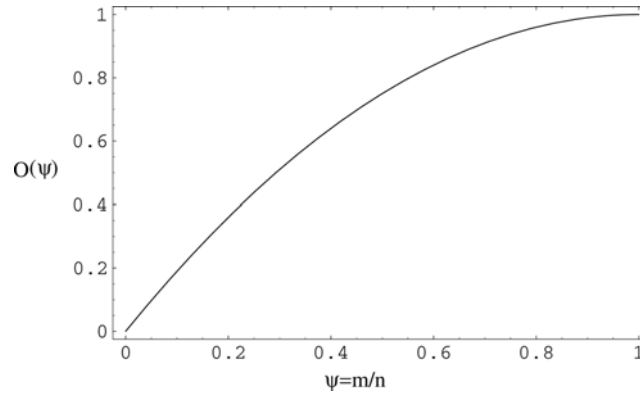


Fig. 4 Computational effort in dependence on ψ

4. Benchmark examples of soil-structure interaction in the time domain

To demonstrate the accuracy and applicability of the derived procedure three numerical examples are presented. These examples have been studied by von Estorff and Prabucki (1990) as a benchmark for their coupled FEM/BEM formulation and can be easily compared to the presented method.

4.1 Semi-infinite rectangular domain with vertical load

For the first example a semi-infinite domain with a time-dependent vertical load is considered. Fig. 5 illustrates the elastic region with applied load, load function and location of observation point A .

The elastic region (plane strain) has a Young's modulus $E = 2.66 \cdot 10^5 \text{ kN/m}^2$, Poisson's ratio

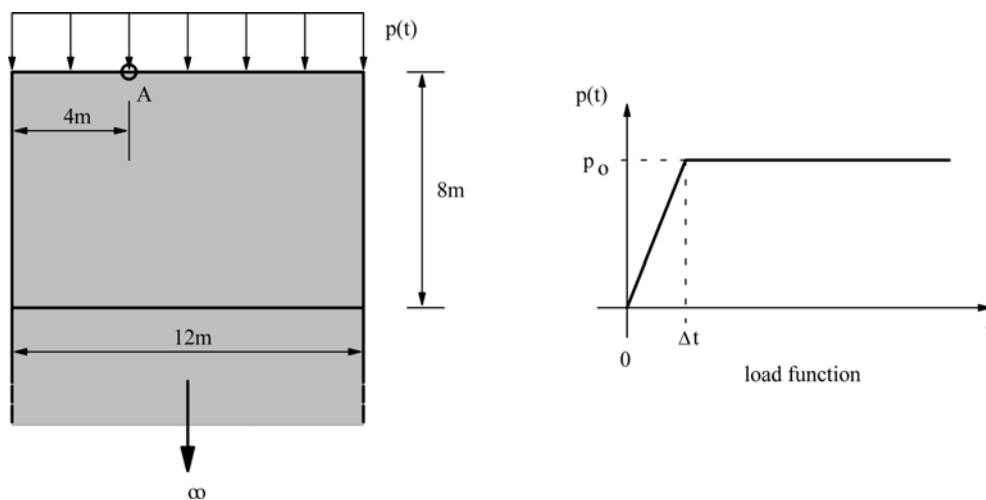


Fig. 5 Semi-infinite rectangular domain (system and load function)

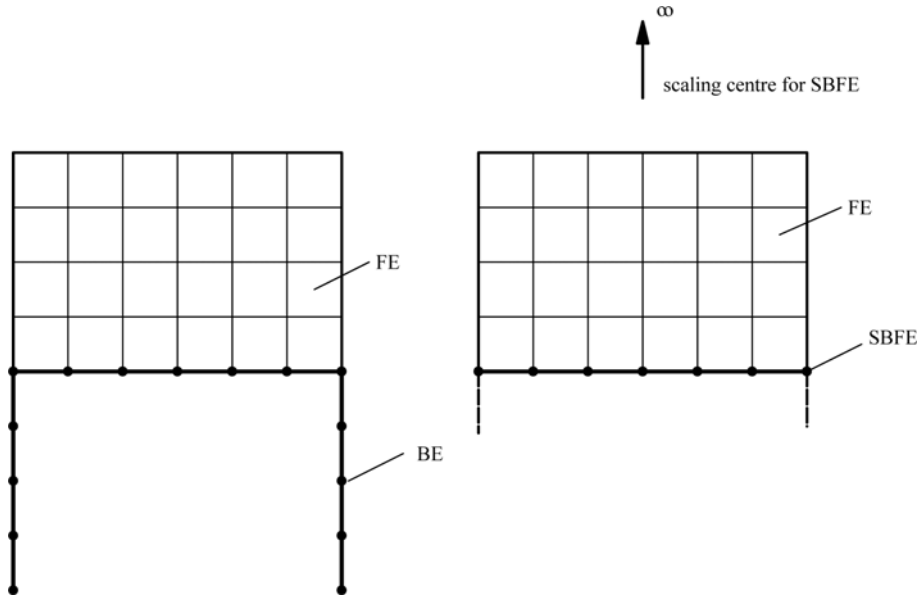


Fig. 6 Semi-infinite rectangular domain (FE/BE and FE/SBFE discretisation)

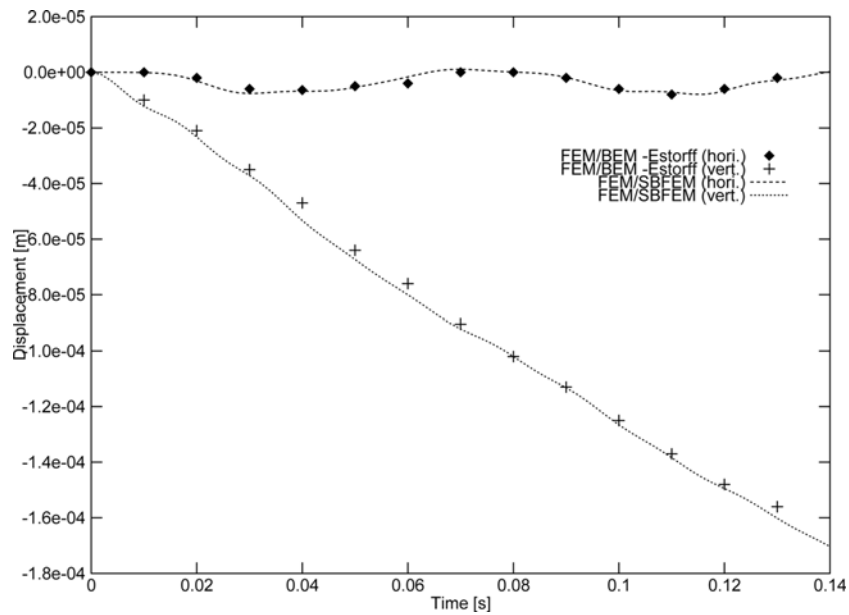


Fig. 7 Semi-infinite rectangular domain (displacement of point *A* due to a vertical load – coupled FE/BE and FE/SBFE approach)

$\nu=0.33$ and a density $\rho=2.0 \cdot 10^3 \text{ kg/m}^3$. The discretisation of this problem with linear finite and boundary elements, and linear scaled boundary finite elements is shown in Fig. 6. A time-step $\Delta t=0.002s$ was chosen for all benchmark examples. The calculated horizontal and vertical displacements of point *A* are studied.

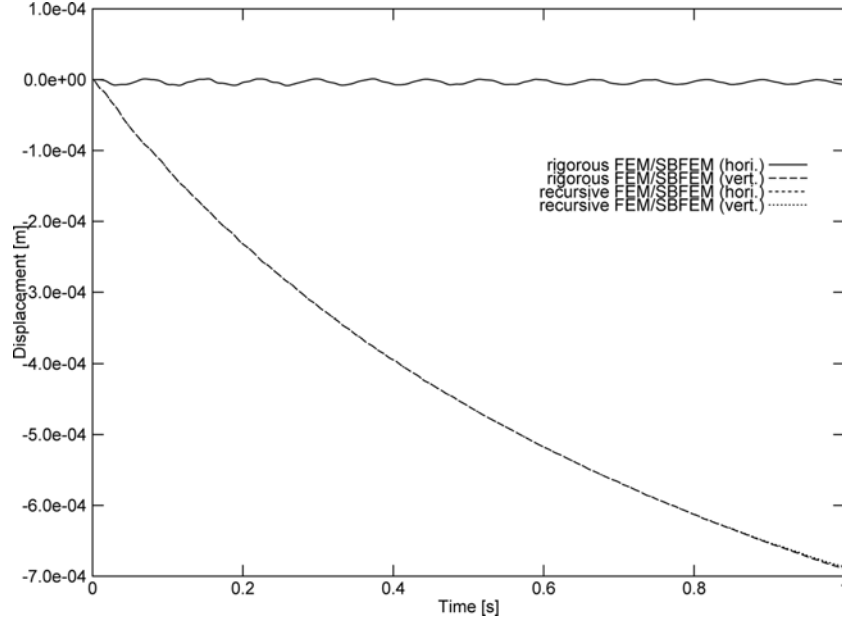


Fig. 8 Semi-infinite rectangular domain (displacement of point A due to a vertical load - coupled FE/SBFE approach, rigorous and recursive algorithm)

Fig. 7 shows the displacement of point A , for a time interval $0 \leq t \leq 0.14s$, calculated with a coupled FE/BE method, and a coupled FE/SBFE method. The results show excellent agreement for the calculated horizontal displacement, as well as for the vertical displacement of observation point A . Notice that the scaling centre for the scaled boundary transformation lies in infinite distance to the finite element/scaled boundary finite element interface, because the semi-infinite domain has parallel sides.

Fig. 8 depicts the results of a coupled finite element/ scaled boundary finite element approach for a longer simulation time ($0 \leq t \leq 1s$). A rigorous ('conventional') calculation is compared with the presented recursive algorithm. The results show excellent agreement of rigorous and recursive algorithm, no differences can be observed.

The time-step m from which on a linear development of the unit impulse response matrix is assumed, was found to be $m = 80$ (corresponding time $t = 80 \cdot 0.002s = 0.16s$). According to Eqs. (17) and (18), the computational effort is reduced to 0.294, compared to the rigorous algorithm, so the reduction of necessary operations (equivalent to CPU time consumption) is 70.6%.

4.2 Response of an elastic half-space

For the second example an infinite half-space with a time-dependent horizontal load is considered. Fig. 9 shows the load and two observation points (A and B) on the surface of the elastic half-space. The material properties are the same as for the first example. Fig 10 shows the time-dependent horizontal load $p(t)$, called Ricker-wavelet, where $p(t)$ is given by:

$$p(t) = (1 - 2\tau^2)\exp(-\tau^2) \quad \text{where} \quad \tau = t\pi - 3 \quad (19)$$

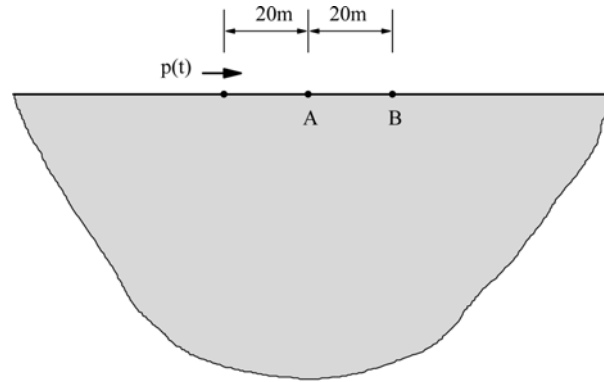


Fig. 9 Elastic half-space (location of load and observation points)

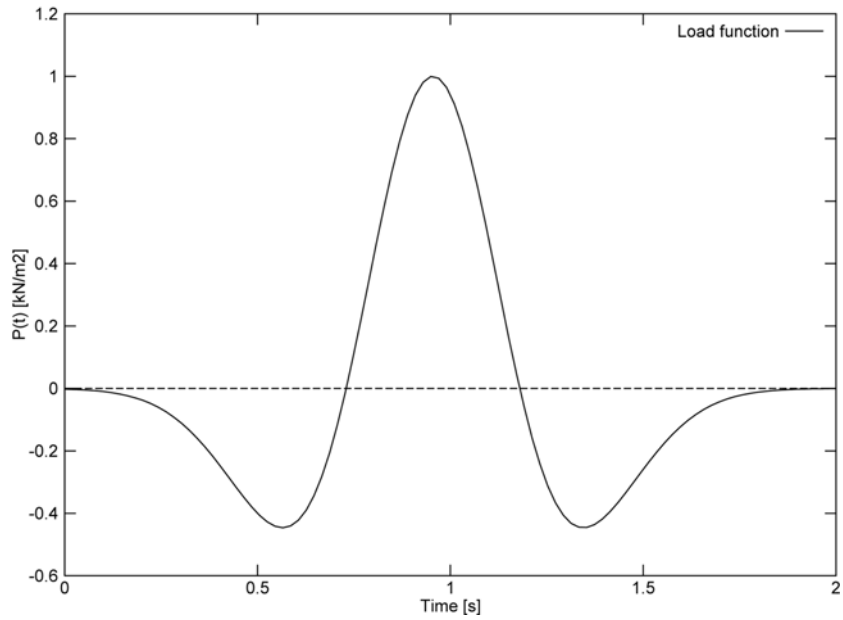


Fig. 10 Load function $p(t)$ (Ricker wavelet)

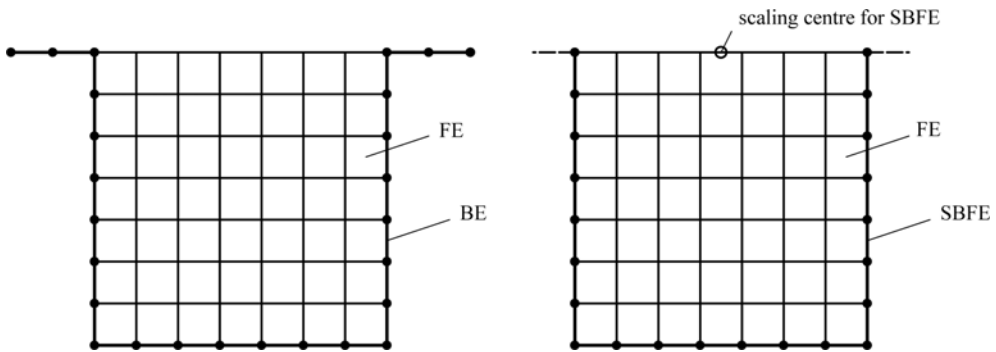


Fig. 11 Elastic half-space (FE/BE and FE/SBFE discretisation)

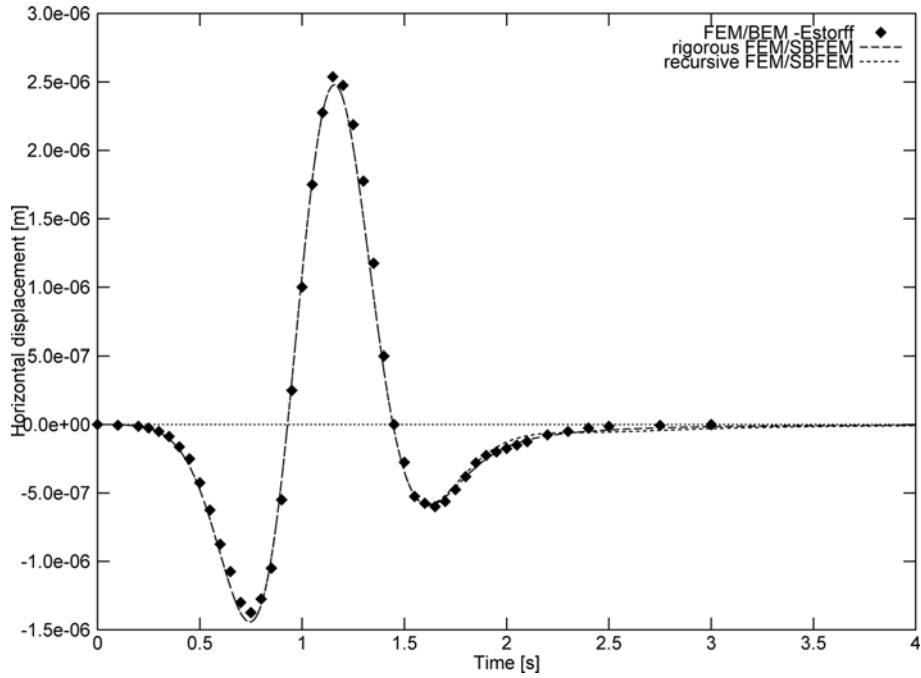


Fig 12 Elastic half-space (horizontal displacement of point A due to horizontal load $p(t)$ – coupled FE/BE approach and coupled FE/SBFEM approach, rigorous and recursive algorithm)

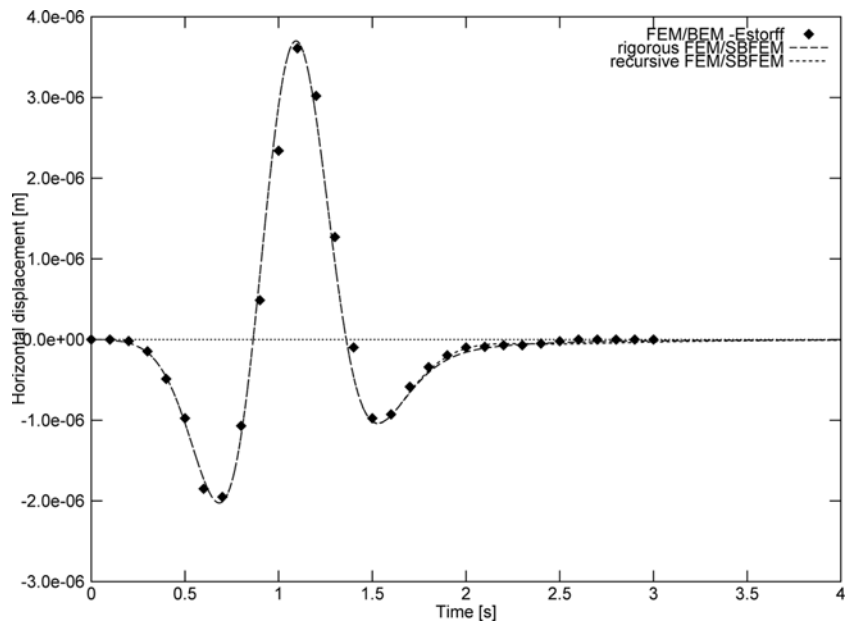


Fig 13 Elastic half-space (horizontal displacement of point B due to horizontal load $p(t)$ – coupled FE/BE approach and coupled FE/SBFEM approach, rigorous and recursive algorithm)

The discretisation, again of a coupled FE/BE and a FE/SBFE system is shown in Fig. 11. Here, the scaling centre for the scaled boundary approach lies inside the FE domain, on the surface of the infinite half-space. For the coupled FE/SBFE approach only the scaled boundary finite elements on the near-field/far-field interface are necessary, while for the FE/BE discretisation a few additional boundary elements on the surface of the half-space on both sides of the finite element mesh must be placed.

The results of the calculation (horizontal displacement of point *A* and *B*) are shown for both approaches in Figs. 12 and 13. Again, an excellent agreement between the coupled FE/BE and FE/SBFE approach is obvious, also for the recursive algorithm. The simulation time *t* is 4s. For the recursive algorithm $m = 309$ is found, so with $\Delta t = 0.002s$ ($n = 2000$) the computational effort is reduced to 0.285 compared to the rigorous algorithm, so the reduction of necessary operations (equivalent to CPU time consumption) is 71.5%. For both examples, the reduction of CPU time consumption due to the recursive algorithm is huge, while nearly no loss of accuracy can be observed.

5. Conclusions

Soil-structure interaction in the time domain is a computationally intensive task. Consequently, it is desirable to develop efficient numerical procedures for engineering problems. The computational effort can be dramatically reduced to an acceptable level with marginal loss of accuracy by using the presented recursive algorithm in conjunction with the Scaled Boundary Finite Element Method. This algorithm is based on an approximation of the unit impulse response matrices by linear time dependence after a certain time-step. This approximation results in an efficient scheme for the evaluation of the involved convolution integral. The comparison with a coupled FE/BE approach shows excellent agreement.

But further approximations in space should be made for another reduction of computational costs (see, e.g., Zhang *et al.* 1999), to enable an analysis of large three-dimensional domains, also with non-linear material behaviour in the near-field.

The presented coupled SBFE approach is easy to incorporate in any Finite Element code, while the symmetry of the system matrices will not be destroyed. If additional approximation in space will be made, the sparse structure of the matrices will be kept as well.

Finally, it can be stated that the practical relevance of the presented approach can be considered to be high.

References

- Antes, H. and Spyrakos, C.C. (1997), *Soil-structure Interaction*, Editor: Beskos, D.E.; Anagnostopoulos, S.A., Computer Analysis and Design of Earthquake Resistant Structures.
- Bettess, P. (1992), *Infinite Elements*, Penshaw Press, Sunderland, U.K..
- Bonnet, M., Maier, G. and Polizzotto, C. (1998), "Symmetric Galerkin boundary element methods", *ASME, Appl. Mech. Rev.*, **51**(11), 669-703.
- Coifmann, R., Rokhlin, V. and Wandzura, S. (1993), "The fast multipole method for the wave equation: A pedestrian prescription", *IEEE, Antennas and Propagation Magazine*, **35**(3), 7-12.
- Crouch, R.S. and Bennett, T. (2000), "Efficient EBE treatment of dynamic far-field in non-linear FE soil-

- structure interaction analyses”, *Proc. of ECCOMAS 2000*, European Congress on Computational Methods in Applied Sciences and Engineering, Barcelona.
- Dasgupta, G. (1982), “A finite element formulation for unbounded homogeneous continua”, *J. Appl. Mech.*, ASME, **49**, 136-140.
- Deeks, A. and Wolf, J.P. (2002), “An h -hierarchical adaptive procedure for the scaled boundary finite element method”, *Int. J. Num. Meth. Eng.*, **54**, 585-605.
- Enquist, B. and Majda, A. (1977), “Absorbing boundary conditions for the numerical simulation of waves”, *Math. of Computation*, **31**(139), 629-651.
- Eringen, A.C. and Suhubi, E.S. (1975), *Elastodynamics, Volume II, Linear Theory*, Academic Press, New York.
- Estorff, O.V. and Firuziaan, M. (2000), “Coupled BEM/FEM approach for nonlinear soil/structure interaction”, *Eng. Anal. with Boundary Elements*, **24**, 715-725.
- Estorff, O.V. and Prabucki, M.J. (1990), “Dynamic response in the time domain by coupled boundary and finite elements”, *Comp. Mech.*, **6**, 33-46.
- Gould, P.L. (1994), *Introduction to Linear Elasticity*, Springer, Berlin.
- Lehmann, L. (2003), “Schnelles Verfahren zur Berechnung der Baugrund-Bauwerk-Interaktion im Zeitbereich”, *D-A-CH Mitteilungsblatt*, **22**(3), 6-9.
- Lehmann, L., Antes, H. and Schanz, M. (2004), “Transient analysis of soil-structure interaction problems: An effective FEM/SBFEM approach”, *Proc. of Advanced Numerical Analyses of Solids and Structures, and Beyond*, 99-116, TU Graz, Austria
- Liao, Z.P. and Wong, H.L. (1984), “A transmitting boundary for the numerical simulation of elastic wave propagation”, *Soil Dyn. Earthq. Eng.*, **3**(4), 174-183.
- Lysmer, J. and Kulmeyer, R.L. (1969), “Finite dynamic model for infinite media”, *J. Eng. Mech.*, ASCE, **95**, 859-875.
- Nishimura, N. (2002), “Fast multipole accelerated boundary integral equation methods”, *Appl. Mech. Rev.*, **55**(4), 299-324.
- Song, C. and Wolf, J.P. (1995), “Consistent infinitesimal finite-element cell method: out of plane motion”, *J. Eng. Mech.*, ASCE, **121**, 613-619.
- Song, C. and Wolf, J.P. (1996a), “Consistent infinitesimal finite-element cell method for diffusion equation in unbounded medium”, *Comp. Methods Appl. Mech. Eng.*, **132**, 319-334.
- Song, C. and Wolf, J.P. (1996b), “Consistent infinitesimal finite-element cell method: three dimensional vector wave equation”, *Int. J. Num. Meth. Eng.*, **39**, 2189-2208.
- Song, C. and Wolf, J.P. (1997), “Consistent infinitesimal finite-element cell method: for incompressible unbounded medium”, *Communications Num. Meth. Eng.*, **13**, 21-32.
- Weber, B. (1994), “Rational transmitting boundaries for time-domain analysis of dam-reservoir interaction”, Dissertation, Inst. of Struct. Eng. of the Swiss Federal Inst. of Tech. (ETH), Zürich, Switzerland.
- Wolf, J.P. and Song, C. (1996), *Finite-Element Modelling of Unbounded Media*, John Wiley & Sons, Chichester, U.K..
- Wolf, J.P. (2003), *The Scaled Boundary Finite Element Method*, John Wiley & Sons, Chichester, U.K..
- Zhang, X., Wegner, J.L. and Haddow, J.B. (1999), “Three-dimensional dynamic soil-structure interaction analysis in the time domain”, *Earthq. Eng. Struct. Dyn.*, **28**, 1501-1524.
- Zienkiewicz, O.C. (1991), *The Finite Element Method*, McGraw-Hill, New York.